Journal Pre-proof

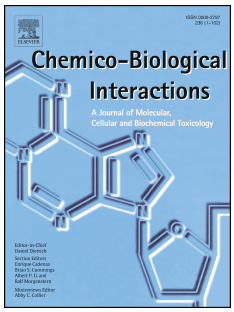

AMPK activation induced by promethazine increases NOXA expression and Beclin-1 phosphorylation and drives autophagy-associated apoptosis in chronic myeloid leukemia

Hyllana C.D. Medeiros, Carina Colturato-Kido, Letícia S. Ferraz, Claudia A. Costa, Vivian W.R. Moraes, Edgar Julian Paredes-Gamero, Ivarne L.S. Tersariol, Tiago Rodrigues

PII: S0009-2797(19)31382-1

DOI: https://doi.org/10.1016/j.cbi.2019.108888

Reference: CBI 108888

To appear in: *Chemico-Biological Interactions*

Received Date: 12 August 2019

Revised Date: 15 October 2019

Accepted Date: 28 October 2019

Please cite this article as: H.C.D. Medeiros, C. Colturato-Kido, Letí.S. Ferraz, C.A. Costa, V.W.R. Moraes, E.J. Paredes-Gamero, I.L.S. Tersariol, T. Rodrigues, AMPK activation induced by promethazine increases NOXA expression and Beclin-1 phosphorylation and drives autophagy-associated apoptosis in chronic myeloid leukemia, *Chemico-Biological Interactions* (2019), doi: https://doi.org/10.1016/j.cbi.2019.108888.

AMPK activation induced by promethazine increases NOXA expression and Beclin-1 phosphorylation and drives autophagy-associated apoptosis in chronic myeloid leukemia

*Hyllana C D Medeiros[1], Carina Colturato-Kido[1], Letícia S Ferraz[1], Claudia A Costa[2], Vivian W. R. Moraes[3], Edgar Julian Paredes-Gamero[4], Ivarne L S Tersariol[5], Tiago Rodrigues[1]**

[1]Center for Natural and Human Sciences (CCNH), Federal University of ABC (UFABC), Santo André, SP, Brazil.
[2]Interdisciplinary Center of Biochemistry Investigation (CIIB), University of Mogi das Cruzes (UMC), Mogi das Cruzes, SP, Brazil.
[3]Department of Molecular Medicine, The Scripps Research Institute, La Jolla, CA, USA.
[4]School of Pharmaceutical Sciences, Federal University of Mato Grosso do Sul (UFMS), Mato Grosso do Sul, Campo Grande, MS, Brazil.
[5]Department of Biochemistry, São Paulo School of Medicine, Federal University of São Paulo (Unifesp) São Paulo, SP, Brazil.

***Corresponding author:** Prof. Tiago Rodrigues, Ph.D. Center for Natural and Human Sciences, Federal University of ABC, UFABC. Avenida dos Estados, 5001. Bloco A, Torre 3, Sala 623, Santo André, SP, Brasil. CEP 090210-580. Santo André, SP. Brasil. e-mail: tiago.rodrigues@ufabc.edu.br.

Short Title. Promethazine-induced leukemia cell death.

Keywords: Autophagy; Cell Death; Drug Repurposing; Leukemia; Phenothiazine.

Highlights

1. Resistance to chemotherapy is a clinical challenge in leukemia therapy.
2. Antiallergic small molecule promethazine is used as antiemetic in cancer patients.
3. Promethazine induced a selective leukemia cell death through autophagy-apoptosis.
4. For the first time, the antitumor effects of promethazine were described.

Graphical Abstract

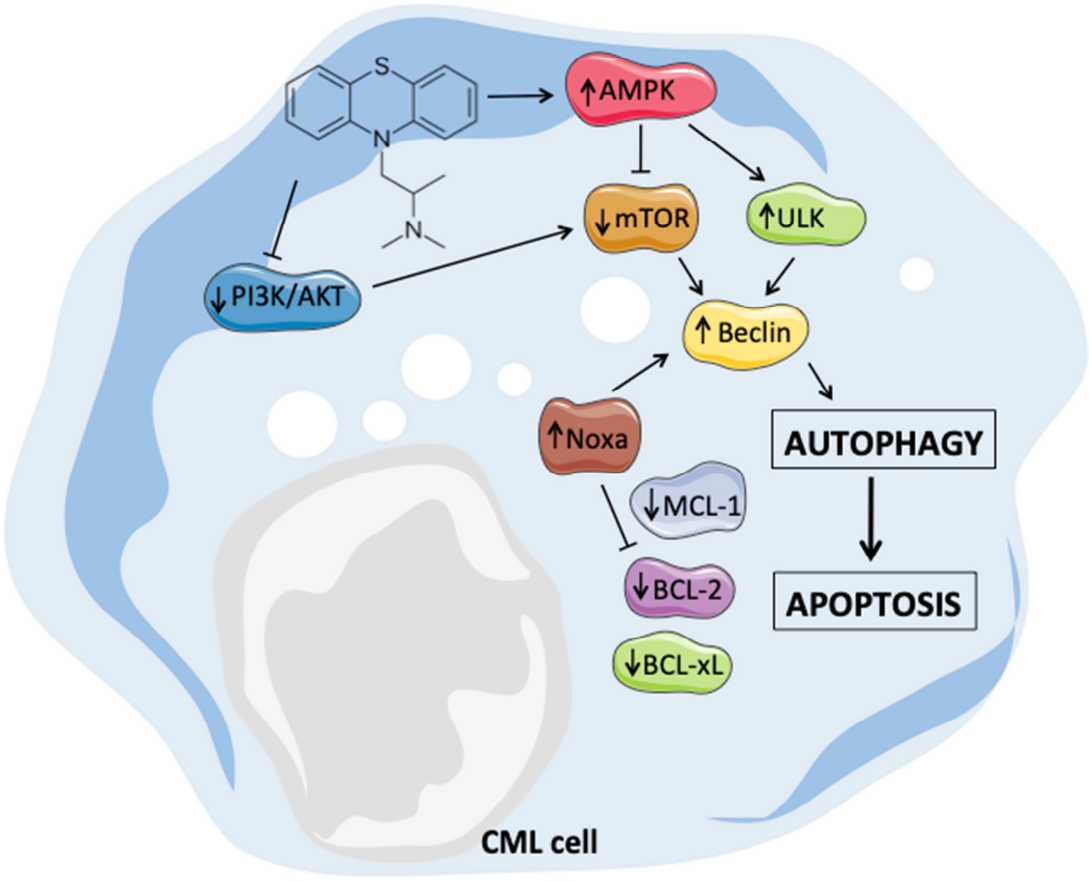

Abstract

Relapse and drug resistance is still major challenges in the treatment of leukemia. Promethazine, an antihistaminic phenothiazine derivative, has been used to prevent chemotherapy-induced emesis, although there is no report about its antitumor potential. Thus, we evaluated the promethazine cytotoxicity against several leukemia cells and the underlying mechanisms were investigated. Promethazine exhibited potent and selective cytotoxicity against all leukemia cell types *in vitro* at clinically relevant concentrations. Philadelphia positive chronic myeloid leukemia (CML) K562 cells were the most sensitive cell line. The cytotoxicity of promethazine in these cells was triggered by the activation of AMPK and inhibition of PI3K/AKT/mTOR pathway. The subsequent downstream effects were NOXA increase, MCL-1 decrease, and Beclin-1 activation, resulting in autophagy-associated apoptosis. These data highlight targeting autophagy may represent an interesting strategy in CML therapy, and also the antitumor potential of promethazine by acting in AMPK and PI3K/AKT/mTOR signaling pathways. Since this drug is currently used with relative low side effects, its repurposing may represent a new therapeutic opportunity for leukemia treatment.

1. Introduction

Cancer is the second leading cause of death globally and accounted for 8.8 million deaths in 2015. The economic costs of cancer in 2010 were estimated at approximately US$ 1.16 trillion and this number will increase with more than 20 million new cases estimated for 2025 (WHO, 2018). Leukemia is a group of hematological diseases originated from the bone marrow precursor cells and it is divided in different subtypes according to cellular maturity (acute or chronic) and cell type (lymphocytic or myeloid) (Chen et al., 2017).Its incidence is 5.2 cases/100,000 people in the world (GCO, 2018) and chemotherapy is an important therapeutic option, although the specifically treatment will depend on the type of leukemia and the individual age (Gambacorti-Passerini et al., 2014). However, the development of drug resistance results in refractory disease or relapse after an initial response, and the treatment failure (Mathisen et al., 2014; Liu et al., 2016).This represents the major therapeutic challenge to be overcome, implying in the need for discovering new targets and developing more effective drugs to increase the chemotherapy success.

The development and approval of new drugs against cancer is costly and spends long developing time with a high rate of failure. One alternative is to prospect new uses for drugs approved for other diseases, as candidates for cancer treatment (Hernandez et al., 2017). Such strategy has proved to be faster and cheaper, and increasing the therapeutic arsenal against cancer. The great advantage of drug repurposing is the rapidly translation into phase II and III clinical studies, since the pharmacokinetics, pharmacodynamics, and toxicity profiles of drugs are well known (Chen et al., 2016). For example, metformin was originally used to diabetes treatment and it has been studied for its anticancer activity (Fuming et al., 2018). Recent studies have showing that phenothiazine derivatives used in treatment of schizophrenia, psychosis, and anxiety, also

promotes mitochondrial alterations related to cell death (Cruz et al., 2010; De Faria et al., 2015) and exhibits selective cytotoxicity against tumor cells (Gil-Ad et al., 2004; Zhelev et al., 2004; Gutierrez et al., 2014; Mello et al., 2016).

The antiallergic small molecule promethazine (PMTZ) is also a phenothiazine derivative with predominant antagonism on H_1-histaminergic receptors, different from the antipsychotic phenothiazines, which blocks dopaminergic D_2 receptors. Besides the main antihistaminic activity, PMTZ is also used in Medicine as antiemetic and sedative (Baldessarini & Tarazi, 2005). Protective effects of PMTZ have been proposed in several biological models, including inhibition of microsomal lipid peroxidation (Slater, 1968) and mitochondrial permeability transition pore (Tarkkila et al., 1995). Also, neuro and hepatoprotective effects reported for PMTZ were attributed to the ability to prevent mitochondrial dysfunctions (An et al., 2017; Geng et al., 2017), apparently without affecting cellular bioenergetics and cell proliferation (Poteet et al., 2013). Interestingly, PMTZ has been used for prevention and treatment of nausea and vomiting induced by antitumor chemotherapeutic drugs, such as cisplatin and paclitaxel, and in the adjuvant treatment of oncologic patients as a sedative or sleep aid (Federico et al., 1990). Considering PMTZ has already being used in cancer patients in order to diminished the side effects of chemotherapy, this study aimed to investigate possible cytototoxicity exhibited by PMTZ against leukemia cells and underlying mechanisms. PMTZ exhibited potent and selective cytotoxicity against different types of leukemia cells *in vitro* by triggering autophagy-mediated apoptotic cell death. Further studies are needed to evaluate its *in vivo* action in a xenograft tumor model. Thus, for the first time, these findings highlight the pharmacological potential of antiallergic promethazine as possible adjuvant drug and also autophagy as a target in leukemia chemotherapy.

2. Materials and methods

2.1.Cell culture and standard incubation conditions

The cell lines used in this study were Jurkat (acute lymphoblastic leukemia), Jurkat BCL-2(acute lymphoblastic leukemia over expressing BCL-2 antiapoptotic protein), ARH-77 (plasma cell leukemia), CCRF-CEM (acute lymphoblastic leukemia), KG-1 (acute myelogenous leukemia), Raji-1 (Burkitt's lymphoma), K562 (chronic myelogenous leukemia), and Lucena-1 (chronic myelogenous leukemia, vincristine resistant). All cell lines were tested mycoplasma-free by indirect staining with Hoechst 33258 (Thermo Fisher Scientific, MA, USA). Cells were grown in RPMI 1640 (Sigma Chem. Co., St. Louis, MO, USA), pH 7.4, supplemented with 10% (v/v) fetal bovine serum (Gibco, Invitrogen, MA, USA), 100 U/mL penicillin and 100 μg/mL streptomycin, in a 5% CO_2 atmosphere at 37°C (Panasonic MCO-19AIC,Japan). For the experiments, cells (1×10^5 cells/mL) were centrifuged ($160\times g$ for 10 minutes), and suspended in supplemented RPMI 1640 medium. Cells were pippeted into microplate wells followed by the addition of different concentrations of PMTZ (Selleckchem, TX, USA).

2.2.Cytotoxicity assays

PMTZ cytotoxicity was screened by the MTT reduction test against several leukemia tumor cell lines (Jurkat, Jurkat BCL-2, ARH-77, CCRF-CEM, KG-1, Raji-1, K562, and Lucena-1), and also against human peripheral blood mononuclear cells (PBMC) for comparative purposes with normal cells. Cells were seeded in 96 multiwell plates (1×10^5/mL) and PMTZ added at increasing concentrations followed by24hincubation. After this, 0.25 mg/mL MTT was added and incubated for 4 h. Then, 0.1 mL of 10 % (w/v) SDS solution was added, incubated overnight, and plates were read at 570 nm and 620 nm, as background (Biochrom Asys Expert Plus

Microplate Reader, Biochrom Ltd., Cambridge, UK). The modulators (50 µM Boc-D-FMK, 60 µM necrostatin-1, 20 µM NSCI, 5 mM 3-methyl adenine (3-MA), 20 µM LY294002, and 1mM N-acetyl cysteine (NAC), all from Sigma-Aldrich, UK) were preincubated 1 h before the addition of PMTZ. For the experiment with PMBC, a human blood sample (5 mL) was collected, mixed with equal volume of supplemented RMPI 1640 medium and Ficoll medium (Life Sciences, USA). After centrifugation at 1,100×*g* for 20 minutes, PBMC layer was collected, suspended in supplemented RMPI 1640 medium, and centrifuged again at 750×*g* to remove the remaining Ficoll solution. Platelets were separated from PBMCs by centrifugation at 150×*g* for 10 minutes. PBMC were collected in supplemented RMPI 1640 medium, stimulated with phytohemagglutinin (5.0 µg/mL), and submitted to MTT assay after 24h incubation with 25 and 50 µM PMTZ. The Human Research Ethics Committee of Federal University of ABC approved the experiment under protocol number 00955018.8.0000.5594. Additionally, PMTZ cytotoxicity was evaluated by the trypan blue exclusion assay in K562 and Lucena-1 cell lines in order to exclude any redox interference of PMTZ with the MTT assay. To do this, after incubation with increasing PMTZ concentrations for 24 h, 0.016 % (w/v) trypan blue was added and cells were counted in a Neubauer's chamber. Cell viability in both assays was calculated in relation to the control (absence of PMTZ), considered as 100%. EC_{50} values were calculated as described (De Faria et al., 2015).

*2.3.**Annexin V-FITC/PI staining***

After incubation with PMTZ for 24 h, K562 cells were centrifuged (160×*g* for 10 minutes) and suspended in 50 µL of binding buffer (Moraes et al., 2013) plus 5 µL of Annexin V-FITC (BD Biosciences, CA, USA) and 5 µL of propidium iodide (PI) (BD Biosciences, USA). The mixture was incubated in the dark at room temperature for 20 minutes, and after addition of 0.3 mL of

binding buffer, fluorescence emission was acquired in a FACSCanto II Flow Cytometer (BD Biosciences), acquiring 10,000 events per sample using Coherent® Sapphire™ 488-20 solid state blue laser with excitation at 488 nm, dichroic mirror 502LP, bandpass filter 530/30 for FITC fluorescence channel and dichroic mirror 556LP, bandpass filter 585/42 for PI fluorescence channel. Data analyses and graphs were performed with Flow Jo vX.0.7 software (Ashland, OR, USA).

2.4.Propidium Iodide (PI) / Hoechst 33342 double staining

After incubation with PMTZ for 24 h, K562 cells were centrifuged (160×*g* for 10 minutes) and suspended in 0.3 mL of RPMI 1640 medium plus 8µM Hoechst 33258 (Thermo Fisher Scientific, MA, USA) and 1.5 µM PI for 30 min. Fluorescence emission was acquired in a widefield fluorescence microscopy system Leica AF6000 (Leica Microsystems, Germany) using the cube filters A4 (Ex: 360/40, dichroic mirror: 400 nm: Filter BP: 470/40) and Y3 (Ex: 545/40, dichroic mirror: 565 nm, BP filter: 610/38), objective lens HCX PL FLUOTAR 63X/1.25n.a. OIL, and camera DFC365FX (Leica Microsystems, Germany).

2.5.Mitochondrial membrane potential (ΔΨ) estimation

After incubation with PMTZ for 24 h, K562 cells were centrifuged (160×*g* for 10 minutes) and suspended in 1.0 mL of PBS containing 20 nM TMRM (Thermo Fischer Scientific, MA, USA). The mixture was incubated in the dark at 37°C for 30 minutes, centrifuged (160×*g* for 10 minutes), and suspended in 0.3 mL of PBS.As positive control, 50 µM CCCP (carbonyl cyanide 3-chlorophenylhydrazone) was used to dissipate the mitochondrial potential. Fluorescence emission was detected in a FACSCanto II Flow Cytometer (BD Biosciences, CA, USA), acquiring 10,000 events per sample using dichroic mirror 556LP, bandpass filter 585/42 nm for

168 TMRM fluorescence channel. Data analyses and graphs were performed with Flow Jo vX.0.7
169 software (Ashland, OR, USA).

170 ***2.6.ROS production***

171 After incubation with PMTZ for 24 h, K562 cells were centrifuged (160×*g* for 10 minutes) and
172 suspended in 1.0 mL of PBS containing 10 µM CM-H_2DCFDA (Life Technologies, Invitrogen,
173 USA). The mixture was incubated in the dark at 37°C for 30 minutes, centrifuged (160×*g* for 10
174 minutes), and suspended in 0.3 mL of PBS. As positive control, it was used 100 µM hydrogen
175 peroxide (H_2O_2). Fluorescence emission was detected in a FACSCanto II Flow Cytometer (BD
176 Biosciences, CA, USA), acquiring 10,000 events per sample using Coherent® Sapphire™ 488-
177 20 solid state blue laser with excitation at 488 nm, dichroic mirror 502LP, bandpass filter 530/30
178 for FITC fluorescence channel. Data analyses and graphs were performed with Flow Jo vX.0.7
179 software (Ashland, OR, USA).

180 ***2.7.Western blotting***

181 After incubation with PMTZ for 6, 12, and 24 h, K562 cells were lysed with RIPA buffer 1X
182 (Thermo Fischer Scientific, MA, USA) with 1X protease/phosphatase inhibitor cocktail (Cell
183 Signaling, MA, USA) and 200 nM PSMF (Cell Signaling, MA, USA). The protein concentration
184 was determined using the Lowry method (Lowry et al., 1951). Briefly, aliquots (20-60 µg) of
185 total cell lysates were resolved using SDS–PAGE gels, blotted onto nitrocellulose membranes
186 (Bio-Rad, CA, USA), and blocked with a solution of 2.5% BSA in Tris-buffered saline with
187 Tween 20 (150 mM NaCl, 2.5 mM KCl, 0.05% Tween 20 (v/v) in 0.025 M Tris HCl, pH 7.4).
188 Proteins were subsequently detected using the following primary antibodies diluted 1:1000,
189 Ambra1 (#24907), AMPKα (#58320), ATG5 (#12994), ATG7 (#8558), BAX (#5023), BCL-2

(#15071), BCL-XL (#2764),BIM (#2933), Caspase-8 (#4790), LAMP2 (#49067), LC3 A/B (#12741), mTOR (#2983), NOXA (#14766), Phospho-Beclin-1 (#13825), Phospho-MCL-1 (#4579), Phospho-mTOR (#2971), Phospho-PI3Kinase (#4228), Phospho-SQSTM1/p62 (#13121), SQSTM1/p62 (#8025), ULK1 (#8054), β-Actin (#3700) (Cell Signaling, CA, USA); Beclin-1 (# 612112), PI3-Kinase (#610045) (BD Bioscience, CA, USA), followed by1 h incubation with the respective secondary antibodies diluted 1:10,000, namely, anti-mouse (#7076) or anti-rabbit (#7074) (Cell Signaling, CA, USA), conjugated to horseradish peroxidase. Labeled proteins were detected using the chemiluminescent detection kit Pierce™ ECL Plus Substrate (Thermo Fischer Scientific, A, USA) and acquired with ChemiDoc™ MP Imaging system v5.0 (Bio-Rad, CA, USA).

2.8.Live cell imaging

After incubation with PMTZ for 24 h, K562 cells were centrifuged (160×*g* for 10 minutes) and suspended in 1.0 mL of PBS. Lysosomes were stained with 400 nM Lyso Tracker Green (Thermo Fisher Scientific, MA, USA) and nuclei with 5.0 nM Hoechst 33258 (Thermo Fisher Scientific, MA, USA) for 30 min in the dark. Fluorescence emissions were acquired in a widefield fluorescence microscopy system Leica AF6000, using the set of cube filters A4 (Ex: 360/40, dichroic mirror: 400 nm: Filter BP: 470/40) and L5 (Ex: 480/40, dichroic mirror: 505 nm, BP filter: 527/30), objective lens HCX PL FLUOTAR 63X/1.25na OIL, and camera DFC365FX (Leica Microsystems, Germany).

2.9.Statistical analyses

Values were obtained from at least three independent experiments run in triplicate. Data were expressed as mean ± SEM and the statistical analyses were performed by one-way analysis of

variance, followed by Tukey *post hoc* test, with significance defined as *p<0.05, **p<0.01, *** p<0.001.

3. Results

3.1. Promethazine exhibits potent and selective cytotoxicity against a panel of leukemia cells

The chemical 2D-structure of promethazine (PMTZ) is presented in Fig. 1A. Its cytotoxicity was preliminarily screened by incubating eight different leukemia cell lines (detailed in Materials and Methods) with increasing concentrations of PMTZ (0-200 µM) for 24 h. As observed in Fig. 1B, PMTZ exhibited high cytotoxicity against all different types of leukemia cell lines evaluated, even against the vincristine-resistant chronic mieloyd leukemia (CML) cell, Lucena-1, and also the overexpressing BCL-2 antiapoptotic protein, Jurkat. In order to establish cell type sensitivity and the potency order, half maximal effective concentration (EC_{50}) values were calculated from these concentration-response curves and presented as bar graph (Fig. 1C). The comparative analysis of EC_{50} values revealed that human CML cell line, K562, was the most sensitive to the cytotoxic activity of PMTZ, being selected for the further experiments. In order to exclude a possible redox interference of the drug with the MTT assay, PMTZ cytotoxicity was also evaluated by the trypan blue exclusion assay, using both K562 and Lucena-1 cells. As observed in Fig. 1D, results were similar to that obtained in the MTT assay. Still, the PMTZ-induced cell death was evaluated by flow cytometry using the frontal dispersion of the laser (forward scatter, FSC) that provides information about the relative cell size, and the side scatter (SSC) that is related to granularity or complexity of the cell. PMTZ decreased cell size and increased the

granularity of K562 cells (Fig. 1E), suggestive of a dead cell population quantified in Fig. 1F. Fluorescence microscopy analyses of K562 cells incubated with the cell permeant nuclear dye Hoechst 33342 (blue) and cell non permeant nuclear dye propidium iodide (red) simultaneously revealed that PMTZ promoted plasma membrane permeabilization, as evidenced by the red staining increase at 50 µM PMTZ (Fig. 1G). Interestingly, the comparison of the cytotoxicity of PMTZ between leukemia K562 cells and peripheral mononuclear blood cells revealed specificity, since PMTZ cytotoxicity is higher in tumor than normal cells, as desired for an antitumor chemotherapeutic drug. At 25 and 50 µM, PMTZ decreased the cell viability by 35 and 58%, respectively, without affect significantly the PMBC viability (Fig. 1H).

3.2. Altered expression of Bcl-2 family proteins related to the PMTZ-induced apoptosis

Flow cytometric analyses using annexin V-FITC/PI assay revealed a doubly stained cell population (annexin V^+/PI^+) after incubation of K562 cells with increasing concentrations of PMTZ, indicating an early phosphatidylserine externalization followed by later plasma membrane permeabilization (Fig. 2A). The quantification of apoptotic cells, i.e., annexin V-FITC positive cells, considering all replicates, is presented in Fig. 2B. Despite this, it was not observed caspase 8 (extrinsic pathway) or executioner caspase 3 activation, which is suggestive of a caspase-independent cell death (Fig. 2C). Accordingly, the pan caspase inhibitor Boc-Asp(OMe)-fluoromethyl ketone(Boc)and the caspase 3 inhibitor 1-(4-methoxybenzyl)-5-[2-(pyridin-3-yl-oxymethyl)pyrrolidine-1-sulfonyl]-1H-indole-2,3-dione (NSCI) did not prevented cell death elicited by PMTZ (Fig. 2D and 2E).Considering that necroptosis as a regulated and caspase independent cell death type, necrostatin-1, a RIPK1 inhibitor, was tested and exerted no effect on PMTZ induced cell death (Fig. 2F). Bcl-2 members are well known players in the apoptotic process and alterations in their expression, such as Bcl-2 overexpression, are associated

with chemotherapy failure in leukemia (Reed, 1997). Thus, the effects of PMTZ on Bcl-2 family proteins expression were evaluated by Western blotting. As observed in the Fig. 3A, PMTZ decreased the expression of the anti-apoptotic members, BCL-2, BCL-XL, and MCL-1, whereas increased the expression of pro-apoptotic members BAK and NOXA, deregulating the balance between pro- and anti-apoptotic Bcl-2 members, triggering apoptosis[26-29]. Since a representative analysis was presented for each protein, the quantification of all experimental replicates were presented in the supplementary material (Fig. S1). The significant increase in the NOXA/MCL-1ratio by PMTZ (Fig. 3B), suggests the involvement of mitochondrial dysfunction contributing to the observed cell death, evidenced by the concentration-dependent dissipation of the mitochondrial transmembrane potential induced by PMTZ in K562 cells (Fig. 3C and 3D). The disappearance of TMRM fluorescence observed at 50 μM PMTZ probably is due to the complete disruption of the cells and the fluorophore was diluted in the incubation buffer. The protonophoric uncoupler CCCP was used as positive control in this experiment.

3.3.Promethazine induces autophagy-associated apoptosis in CML K562 cells

Besides its effect on apoptotic signaling, increased expression of NOXA is reported to promote autophagy-mediated cell death, preventing the interaction between MCL-1 and Beclin-1, a protein required for the autophagosome formation (Elgendy et al., 2011). Considering that PMTZ induced increase in the expression of NOXA and decrease of MCL-1, associated to the increased phosphorylation of Beclin-1, we evaluated the effect of inhibitors of autophagy known to target different steps of the autophagic pathway on PMTZ-induced cell death. It was used 3-methyl adenine (3-MA), a class III PI3K inhibitor, which prevents the nucleation of autophagosomes (Hendil et al., 1990), LY294002, a synthetic PI3K inhibitor (Knight & Shokat, 2007),and E-64, an inhibitor of lysosomal proteases, which diminishes the protein degradation

inside lysosomes (Tanida et al., 2005). As observed in Fig. 3 (E, F, and G), the inhibition of initial or final steps of autophagy diminished the cytotoxicity of PMTZ, showing that, in this case, autophagy is contributing to cell death and not to cell rescue/survival.

3.4.Promethazine-induced autophagic cell death is driven by AMPK activation and PI3K/mTOR inhibition

In order to investigate the signaling pathways involved with autophagy-associated cell death induced by PMTZ, different proteins related to autophagy were evaluated. The scheme shown in parallel with the results in Fig. 4A illustrates the overall alterations promoted by PMTZ in CML K562 cells and the quantification of all experimental replicates for each protein were presented in the supplementary material (Fig. S2). The inhibitory function of mTOR in autophagy is well established (Jung et al., 2010). PMTZ decreased the expression of this protein in K562 cells after 24 h incubation, as well as its active (phosphorylated) form, and then, the downstream autophagic cascade was activated. Such effect of PMTZ on mTOR seemed to be mediated by decreased activation of PI3K III, as observed by the decreased expression of its phosphorylated form, thus depressing the PI3K/AKT/mTOR pathway. In parallel, PMTZ also increased the expression of AMP activated protein kinase (AMPK), which is a key energy sensor that regulates cellular metabolism to maintain energy homeostasis and promotes autophagy (Kim et al., 2011).Increased AMPK associated to decreased mTOR in CML cells incubated with PMTZ resulted in the increased of the expression of ULK. Although, the total content of Beclin-1 and Ambra was not affected by PMTZ, the phosphorylated (and active) form of Beclin-1 was significantly increased, while the expression of ATG5 and ATG7 was decreased. The p62 protein has been associated with autophagic recognition as receptor for degradation of ubiquitinated proteins and organelles (Mizushima et al., 2010). It is localized at sites of

autophagosome formation and it is associated with both the autophagosome localization of LC3, which is lipidated and converted to LC3-II, and ubiquitinated proteins (Johansen & Lamark, 2011). PMTZ induced a significant accumulation of p62 (SQSTM1) and LC3-II. Increased LC3-II levels are related to the stimulation of autophagosome synthesis or the decreased autophagosome degradation. In this regard, LysoTracker Green staining revealed increase number and size of acidic compartments in the presence of PMTZ, indicated by the arrows, suggestive of increased autophagolysosome formation (Fig. 4B). At last, considering AMPK may be activated by reactive oxygen species (ROS), this was evaluated in the same experimental conditions. As observed in the Fig. 4C, 50 μM PMTZ (but not 25 μM) increased ROS production evaluated by DCF fluorescence, and the antioxidant N-acetyl cysteine (NAC) prevented the cytotoxicity of PMTZ (Fig. 4D).

4. Discussion

It has been reported that more than 90% of patients affected by chronic myeloid leukemia (CML) cells present the Philadelphia chromosome, a chimeric *BCR-ABL* gene, which results in constitutive expression of a tyrosine kinase protein related to the pathogenesis of the disease. In this regard, the development of specific kinase inhibitors significantly improved CML treatment and patient prognosis (An et al., 2017; Rossari et al., 2018). However, BCR-ABL tyrosine kinase activity inhibition is no longer sufficient to eradicate the disease. Due to the arising of (multi)drug resistance, early relapse and persistence of leukemia stem cells are obstacles to a successful treatment of leukemia patients using chemotherapy (Pan et al., 2014; Lin et al., 2014;

Giustacchini et al., 2017). Therefore, discovery of novel approaches and effective drugs against sensitive and resistant leukemia tumor cells are expected.

Current attention is given to drug repurposing strategy in the drug development field due the cost, time, and even efficacy advantages (Sleire et al., 2017). In this regard, recent literature have pointing to the efficacy of antipsychotic phenothiazine derivatives as potential alternative drugs to be used in cancer chemotherapy (De Faria et al., 2015; Gil-Ad et al., 2004; Zhelev et al., 2004; Gutierrez et al., 2014; Mello et al., 2016; Ivanov, 2014; Wu et al., 2016; Ravinesh et al., 2017). However, there is no data about the antitumor potential of the antihistamine phenothiazine derivative promethazine. Among the reasons for investigating the antitumor potential of promethazine are its low systemic human toxicity compared to antipsychotic phenothiazines, including minor central nervous system and cardiac side effects (Tsay et al. 2015; Handley et al., 2016). Additionally, pharmacokinetic studies with promethazine revealed that plasma concentration after a single 25 mg oral dose ranged between 2.4 and 18 ng/mL, i.e., 7.5 and 56 µM (TAYLOR et al., 1983). Considering that EC_{50} for cytotoxicity in LMC cells is within the clinically used dosage of PMTZ as antihistaminic drug, it is feasible that cancer patients may have benefits from the use of this drug. However, further studies are necessary to evaluate the effects of PMTZ combined with the current chemotherapy for leukemia *in vitro* and *in vivo*.

Our data revealed that PMTZ exhibits potent cytotoxicity against a wide panel of different leukemia cell types. It was interesting to observe that the overexpression of the antiapoptotic protein BCL-2 in Jurkat cells did not conferred resistance to PMTZ-induced cell death. Also, the overexpression of P-glycoprotein (P-gp) in Lucena-1, as a model of MDR positive CML, increased the EC_{50} values for PMTZ when compared with K562 cells. However, Lucena-1 cells were still sensitive to the drug, maybe due to its ability to reverse a MDR phenotype by acting in

gene expression and also in transport activity (Dönmez et al., 2011). Additionally, the comparison with normal PMBC showed PMTZ exhibit some selectivity to tumor cells when compared to circulating normal blood cells, which was also previously reported by the antipsychotic derivative chlorpromazine (Mello et al., 2016).

Annexin V-FITC and propidium iodide double staining is an assay frequently employed to identify the occurrence of apoptosis in the early and late stages or necrotic events (Rieger et al., 2011). The incubation of K562 CML cells with PMTZ resulted in phosphatidylserine externalization, suggestive of apoptosis. Despite the apparent independence of caspases activation, BCL-2 anti- and proapoptotic proteins were modulated accordingly, including a significant increase in NOXA and BAK levels (Chen et al., 2015). NOXA, a BH3 only member well recognized as inhibitor of the antiapoptotic protein MCL-1, is also involved with autophagy-mediated cell death through the disruption of the interaction between MCL-1 and Beclin-1, which is an important constituent of the PI3K complex, required for the autophagosome formation (Elgendy et al., 2011). Accordingly, PMTZ inhibited PI3K/mTOR pathway, which associated to the AMPK activation, was responsible for the induction of autophagy in CML cells. Promethazine induced oxidative stress in K562 cells directly related to its cytotoxicity and such ROS production may be associated to the AMPK activation (Hinchy et al., 2018). However, further studies are necessary to a better comprehension about how PMTZ activates AMPK. In parallel, a recent study showed that PMTZ modulated PI3K/AKT signaling mild hypothermia model, resulting in neuroprotection (An et al., 2017). It is well established that cancer cells exhibit several adaptive modifications in molecular pathways to gain proliferative advantages and escape from the cell death program. In this regard, PI3K/AKT signaling pathway seems to be constitutively activated in several types of leukemia, including acute and chronic

myeloid leukemia, and inhibition seems to impair the growth of tumor cells (Sujobert et al., 2005; Deng et al., 2017; Zhang et al., 2018; Chen et al., 2018). Here, PMTZ simultaneously increased AMPK and inhibited PI3K/AKT/mTOR signaling pathway triggering autophagy-associated apoptosis.

Also, increased NOXA and decreased MCL-1 and Ambra expression contributed to the Beclin-1 phosphorylation and impairment of the autophagic flux (Mizushima et al., 2010; Lee et al., 2019), with p62 and LC3-II accumulation. It was proposed that p62, together with PINK1 and Parkin, plays an important role in mitochondrial dynamics and mitophagy (Rothfuss et al., 2009; Tolkovsky, 2009; Ivankovic et al., 2016). It was shown that the phenothiazine derivative thioridazine promoted mitochondrial permeabilization associated to tumor cell death (Cruz et al., 2010; De Faria et al., 2015). As expected, considering the structural similarities, PMTZ also affected mitochondrial function in K562 cells and possibly such mitochondrial dysfunction contributed to the autophagy activation of autophagy and cell death. Since p62 critically participates in mitochondria degradation and the induction of mitophagy results in increased transcription and translation of p62 (Ivankovic et al., 2016), the role of mitophagy in PMTZ induced CML cell death will be further investigated.

It was shown that the modulation of autophagy is involved in malignant transformation, tumor progression, and drug resistance through a multitude of mechanisms (Elgendy et al., 2011; Galluzzi et al., 2017). For example, the inhibition of autophagy sensitized AML cells to chemotherapy (Nourkeyhani, et al., 2016), being considered as a potential therapeutic target in this type of leukemia (Folkerts et al., 2017; Jang et al., 2017). This was also observed in CML cells, which were sensitized to TKI inhibitors (Helgason et al., 2013). In K562 cells, the inhibition of autophagy decreased cell proliferation and viability, and also affected CD34

positive CML progenitor cells (Ianniciello et al., 2017). Thus, targeting autophagy seems to represent a promising therapeutic approach in leukemia chemotherapy and PMTZ induced autophagy-associated apoptosis may represent a possible drug repurposing strategy in CML chemotherapy.

5. Conclusions

In summary, our results showed, for the first time, the potent cytotoxicity exhibited by PMTZ in leukemia cells *in vitro*, in a selective way relative to normal cells. Molecular investigations revealed that PMTZ targeted AMPK and PI3K/mTOR pathways resulting in autophagy-associated apoptosis (Scheme 1). Since this drug is already in use to control chemotherapy-induced emesis, probably these cancer patients are receiving the antitumor benefits of promethazine. Together, this study provides a proof of concept for the repurposing of antihistaminic drug promethazine as adjuvant to develop novel therapeutic agents for cancer therapy.

FIGURES

Figure 1. Selective cytotoxicity of promethazine against leukemia cells *in vitro*. Cells were incubated with increasing PMTZ concentrations for 24 h. **(A**) Chemical structure of promethazine. **(B)** Cell viability assessed by the MTT reduction test in a panel of leukemia cell lines. **(C)** EC50 values for PMTZ calculated from the concentration-response curves in (B). **(D)** Cell viability assessed by the trypan blue exclusion in K562 and Lucena-1 cell lines. **(E)** Representative dot plots of cell size and granularity (FSC × SSC parameters) obtained by flow cytometry in K562 cells. **(F)** Quantification of 'dead' cell population based on FSC and SSC data in (E). **(G)** Fluorescence microscopic evaluation of K562 cells stained with Hoechst 33342 and PI incubated with 25 and 50 µM PMTZ (63×magnification, scale bars 10 µm). **(H)** Comparison of PMTZ cytotoxicity in PMBC (normal) and CML K562 cells assessed by the MTT assay. Percentage of viable cells was calculated in relation to control (absence of PMTZ), considered as 100%. Results are presented as mean ± SEM of at least three independent experiments performed in triplicate. *($p<0.05$) and *** ($p<0.001$) indicates statistically significant differences.

Figure 2. Promethazine induces caspase-independent apoptotic cell death in human CML K562 cells. (A) Representative dot plots of the cell death profile analyzed by double staining flow cytometry analysis with annexin V-FITC/PI in K562 cells after 24 h incubation with 25 and 50 µM PMTZ. **(B)** Relative quantification of apoptotic cells (annexin V-FITC positive). **(C)** Western blot analyses for detection of total and cleavedcaspase-3, and total caspase-8 in K562 whole cell lysates incubated with 25 and 50 µM PMTZ for 24 h. Numbers under the bands are the densitometry of the proteins normalized by β-actin. Effects of caspase inhibitors on PMTZ-induced cell death evaluated by MTT reduction in K562 cells after 1 h pre incubation with **(D)**

50 µM Boc-D-FMK, **(E)** 10 µM NSC1, and **(F)** 60 µM necrostatin-1. Results are presented as the mean ± SEM of at least three independent experiments performed in triplicate. *** ($p<0.001$) indicates statistically significant differences and *ns* indicates not significant.

Figure3. Altered expression of apoptosis-related Bcl-2 proteins and mitochondrial permeabilization induced by PMTZ in K562 cells, and the effects of autophagy inhibitors on cell viability. **(A)** Cell lysates obtained from PMTZ-treated K562 cells for 24 h were submitted to Western blot analyses for the anti- and proapoptotic Bcl-2 family proteins. Numbers indicate the densitometric quantification normalized by β-actin. **(B)** Averaged NOXA/MCL-1 ratio PMTZ treatment. **(C)** Representative histogram of the mitochondrial transmembrane potential (ΔΨ) evaluated by changes in TMRM fluorescence by flow cytometry. CCCP (50 µM) was incubated during 1 h prior to the acquisition to be used as positive control to dissipate the mitochondrial potential. **(D)** Quantification of TMRM fluorescence considering all replicates. Effects of autophagy inhibitors on PMTZ-induced K562 cell death after 1h pre incubation with **(E)** 3-MA, **(F)** LY294002, and **(G)** E64. Results are presented as the mean ± SEM of at least three independent experiments performed in triplicate. *($p<0.05$), ** ($p<0.01$), *** ($p<0.001$) indicates statistically significant differences.

Figure 4. Promethazine induces autophagic cell death by activating AMPK and inhibiting PI3K pathways (A) Whole cell lysates from K562 cells treated with 25 and 50 µM PMTZ for 24 h were subjected to Western blot analyses for autophagy downstream pathways proteins. Densitometry measurements, normalized to β-actin are indicated below the corresponding blot. **(B)** Fluorescent microscope images of LysoTracker Green-loaded K562 cells treated with 25 and 50 µM PMTZ for 24 h. Red arrow indicates the infracted acid vacuoles (63× magnification, scale

bars 20 µm). **(C)** Detection of DCF fluorescence by flow cytometry. **(D)** Effect of 1 mM N-acetyl cysteine (NAC) on PMTZ-induced K562 cell death.

Scheme 1. Representative illustration of the promethazine-induced autophagy associated apoptosis in leukemia cells.

Supplementary Material

Fig. S1 – Quantification of the protein levels showed in Fig. 3. The densitometry of each protein normalized by the respective constitutive protein was performed. Results are presented as the mean ± SEM of at least three independent experiments performed in triplicate. *($p<0.05$), ** ($p<0.01$), *** ($p<0.001$) indicates statistically significant differences.

Fig. S2 – Quantification of the protein levels showed in Fig. 4. The densitometry of each protein normalized by the respective constitutive protein was performed. Results are presented as the mean ± SEM of at least three independent experiments performed in triplicate. *($p<0.05$), ** ($p<0.01$), *** ($p<0.001$) indicates statistically significant differences.

Author Contributions

All authors have given approval to the final version of the manuscript. T.R. design the study, including the hypothesis and the experiments, and wrote the paper; H.C.D.M., C.C-K., L.S.F., C.A.C., and V.W.R.M performed the experiments; H.C.D.M., I.L.S.T, and T.R. analyzed the data; E.J.P-G. provided critical reagents and analyzed the data.

Acknowledgments

Lucena-1 cell line was kindly provided by Prof. Dr. Vivian Mary Barral Dodd Rumjanek (UFRJ).

Disclosure statement

Authors declare no potential conflict of interest.

Funding

This work was supported by Brazilian funding agencies FAPESP (2012/12247-8; 2016/07367-5) and CNPq (486760/2013-0). This study was financed in part by the Coordenação de Aperfeiçoamento de Pessoal de Nível Superior – Brasil (CAPES) – Finance Code 001 (Scholarship to H.C.D.M.).

References

An, H., Duan, Y., Wu, D., Yip, J., Elmadhoun, O., Wright, J.C., Shi, W., Liu, K., He, X., Shi, J., Jiang, F., Ji, X., Ding Y. (2017) Phenothiazines enhance mild hypothermia-induced neuroprotection via PI3K/Akt regulation in experimental stroke. Sci. Rep. **7**, 7469.

Baldessarini, R.J., Tarazi, F.I. (2005) Drugs and the treatment of psychiatric disorders. Chapters 17 and 18. In: Brunton, L.L., Lazo, J.S., Parker, K.L., (Goodman and Gilman's. The Pharmacological Basis of Therapeutics. 11th McGraw-Hill; New York).

Chen, H., Wu, J., Gao, Y., Chen, H., Zhou, J. (2016) Repurposing of old drugs towards new cancer drug discovery. Curr. Top. Med. Chem. **16**, 2107–2114.

Chen, S., Liang, H., Yang, H., Zhou, K., Xu, L., Liu, J., Lai, B., Song, L., Luo, H., Peng, J., Liu, Z., Xiao, Y., Chen, W., Tang, H. (2017) Long non-coding RNAs: the novel diagnostic biomarkers for leukemia. Environ. Toxicol. Pharmacol. **55**, 81–86.

Chen, H.C., Kanai, M., Inoue-Yamauchi, A., Tu H.C., Huang, Y., Ren, D., Kim, H., Takeda, S., Reyna, D.E., Chan, P.M., Ganesan, Y.T., Liao, C.P., Gavathiotis, E., Hsieh, J.J., Cheng, E.H.

(2015) An interconnected hierarchical model of cell death regulation by the BCL-2 family. Nat. Cell. Biol. **17**, 1270–1281.

Chen Y, Wang T, Du J, Li Y, Wang X, Zhou Y, Yu X, Fan W, Zhu Q, Tong X, Wang Y. (2018) The Critical Role of PTEN/PI3K/AKT Signaling Pathway in Shikonin-Induced Apoptosis and Proliferation Inhibition of Chronic Myeloid Leukemia. Cell Physiol Biochem. **47**, 981-993.

Cruz, T.S., Faria, P.A., Santana, D.P., Ferreira, J.C., Oliveira, V., Nascimento O.R., Cerchiaro, G., Curti, C., Nantes, I.L., Rodrigues, T. (2010) On the mechanisms of phenothiazine-induced mitochondrial permeability transition: Thiol oxidation, strict Ca^{2+}dependence, and cyt *c* release. Biochem. Pharmacol. **80**, 1284–1295.

De Faria, P.A., Bettanin, F., Cunha, R.L., Paredes-Gamero, E.J., Homem-de-Mello, P., Nantes, I.L., Rodrigues, T. (2015) Cytotoxicity of phenothiazine derivatives associated with mitochondrial dysfunction: a structure-activity investigation. Toxicology **1**, 44–54.

Deng L, Jiang L, Lin XH, Tseng KF, Liu Y, Zhang X, Dong RH, Lu ZG, Wang XJ. (2017) The PI3K/mTOR dual inhibitor BEZ235 suppresses proliferation and migration and reverses multidrug resistance in acute myeloid leukemia. Acta Pharmacol Sin. **38**, 382-391.

Dönmez, Y., Akhmetova, L., İşeri Ö.D., Kars, M.D., Gündüz U. (2011) Effect of MDR modulators verapamil and promethazine on gene expression levels of MDR1 and MRP1 in doxorubicin-resistant MCF-7 cells. Cancer Chemother. Pharmacol. **67**, 823–831.

Elgendy, M., Sheridan, C., Brumatti, G., Martin, J.S. (2011) Oncogenic ras-induced expression of noxa and beclin-1 promotes autophagic cell death and limits clonogenic survival. Mol. Cell. **42**, 23–35.

Federico, M., Sabbatini, R., Piccinini, P., Zironi, S., Piccinini, L., Silingardi V. (1990) Prevention of cisplatin-induced vomiting in patients with cancer. A pilot study with a multiagent protocol. Tumori. **76**, 278–281.

Folkerts, H., Hilgendorf, S., Wierenga, A.T.J., Jaques, J., Mulder, A.B., Coffer, P.J., Schuringa, J.J., Velleng,a E. (2017) Inhibition of autophagy as a treatment strategy for p53 wild-type acute myeloid leukemia. Cell Death Dis, e2927. doi: 10.1038/cddis.2017.317.

Fuming, Z., Huapu, Z., Yi, L., Jingsong, H., Qingzhi, S., Zhen, C. (2018) Metformin and cancer: An existing drug for cancer prevention and therapy. Oncol. Lett. **15**, 683–690.

Galluzzi, L., Baehrecke, E., Ballabio, A., Boya, P., Bravo-San Pedro, J.M., Cecconi, F., Choi, A.M., Chu, C.T., Codogno, P., Colombo, M.I., Cuervo, A.M., et al., (2017) Molecular definitions of autophagy and related processes. EMBO J.**36**, 1811–1836.

Gambacorti-Passerini, C., Brümmendorf, T.H., Kim, D.W., Turkina, A.G., Masszi, T., Assouline, S., Durrant, S., Kantarijan, H.M., Khoury, H.J., Zaritskey, A. et al., (2014) Bosutinib efficacy and safety in chronic phase chronic myeloid leukemia after imatinib resistance or intolerance: Minimum 24□month follow□up. Am. J. Hematol. **89**, 732–742.

Geng, X., Li, F., Yip, J., Peng, C., Elmadhoun, O., Shen, J., Ji, X., Ding, Y. (2017) Neuroprotection by chlorpromazine and promethazine in severe transient and permanent ischemic stroke. Mol. Neurobiol. **54**, 8140–8150.

Gil-Ad, I., Shtaif, B., Levkovitz, Y., Dayag, M., Zeldich, E., Weizman, A. (2004) Characterization of phenothiazine-induced apoptosis in neuroblastoma and glioma cell lines: clinical relevance and possible application for brain-derived tumors. J. Mol. Neurosci. **22**, 189–198.

543 Global Cancer Observatory [internet]. Global Cancer Observatory. [cited 19Jan28]. Available
544 from: http://gco.iarc.fr/, 2018.

545 Giustacchini, A., Thongjuea, S., Barkas, N., Woll, P.S., Povinelli, B.J., Booth, C.A.G., Sopp, P.,
546 Norfo, R., Rodriguez-Meira, A., Ashley, N., Jamieson, L., Vyas, P., Anderson, K., Segerstolpe,
547 A., Qian, H., Olsson-Stromberg, U., Mustjoki, S., Snadberg, R., Jacobsen, S.E.W., Mead, A.J.
548 (2017) Single-cell transcriptomics uncovers distinct molecular signatures of stem cells in chronic
549 myeloid leukemia, Nat. Med. **23**, 692–702.

550 Gutierrez, A., Pan, L., Groen, R.W., Baleydier, F., Kentsis, A., Marineau, J., Grebliunaite R.,
551 Kozakewich, E., Reed, C., Pflumio, F.,Poglio S., Uzan, B., Clemons, P., VerPlank, L., An, F.,
552 Burbank, J., Norton, S., Tolliday, N., Steen, H., Weng, A.P., Yuan, H., Bradner, J.E., Mitsiades,
553 C., Look, A.T., Aster, J.C. (2014) Phenothiazines induce PP2A-mediated apoptosis in T cell
554 acute lymphoblastic leukemia. J. Clin. Invest. **124**, 644–655.

555 Handley, S., Patel, M.X., Flanagan, R.J. (2016) Antipsychotic-related fatal poisoning, England
556 and Wales, 1993–2013: impact of the withdrawal of thioridazine. Clin. Toxicol. (Phila) **54**,
557 471–480.

558 Helgason, G.V., Mukhopadhyay, A., Karvela, M., Salomoni, P., Calabretta, B., Holyoake, T.L.
559 (2013) Autophagy in chronic myeloid leukemia: stem cell survival and implication in therapy.
560 Curr. Cancer Drug Targets **13**, 724–734.

561 Hendil, K.B., Lauridsen, A.M., Seglen, P.O. (1990) Both endocytic and endogenous protein
562 degradation in fibroblasts is stimulated by serum/amino acid deprivation and inhibited by 3-
563 methyladenine. Biochem. J. **272**, 577–581.

564 Hernandez, J.J., Pryszlak, M., Smith, L., Yanchus, C., Kurji, N., Shahani, V.M., Molinski, S.V.
565 (2017) Giving drugs a second chance: overcoming regulatory and financial hurdles in
566 repurposing approved drugs as cancer therapeutics. Front. Oncol. **7**, 273.

Hinchy, E.C., Gruszczyk, A.V., Willows, R., Navaratnam, N.,Hall, A.R., Bates, G., Bright, T.P., Krieg, T., Carling, D., Murphy, M.P. (2018) Mitochondria-derived ROS activate AMP-activated protein kinase (AMPK) indirectly.J. Biol. Chem.**293**, 17208–17217.

Ianniciello, A., Dumas, P.Y., Drullion, C., Guitart, A., Villacreces, A., Peytour, Y., Chevaleyre, J., Brunet de la Grange, P., Vigon, I., Desplat, V., Priault, M., Sbarba, P.D., Ivanovic, Z., Mahon, F.X., Pasquet, J.M. (2017) Chronic myeloid leukemia progenitor cells require autophagy when leaving hypoxia-induced quiescence. Oncotarget**8**, 96984–96992.

Ivankovic, D., Chau, K.Y., Schapira, A.H., Gegg, M.E. (2016) Mitochondrial and lysosomal biogenesis are activated following PINK1/parkin-mediated mitophagy. J. Neurochem. **136**, 388–402.

Ivanov, A.I. (2014) Pharmacological inhibitors of exocytosis and endocytosis: novel bullets for old targets. Meth. Mol. Biol. **1174**, 3–18.

Jang, J.E., Eom, J.I., Jeung, H.K., Cheong, J.W., Lee, J.Y., Kim, J.S., Min, Y.H. (2017) Targeting AMPK-ULK1-mediated autophagy for combating BET inhibitor resistance in acute myeloid leukemia stem cells. Autophagy **13**, 761–762.

Johansen, T., Lamark T. (2011) Selective autophagy mediated by autophagic adapter proteins. Autophagy**7**, 279–296.

Jung, C.H., Ro, S.H., Cao, J., Otto, N.M., Kim, D.H. (2010) mTOR regulation of autophagy. FEBS Lett. **584**, 1287–1295.

Knight, Z.A., Shokat, K.M. (2007) Chemically targeting the PI3 K family. Biochem Soc Trans. **35**, 245–249.

Kim, J.K., Viollet, B.M., Guan, K.L. (2011) AMPK and mTOR regulate autophagy through direct phosphorylation of Ulk1. Nat. Cell. Biol. **13**, 132–141.

590 Lee, E.F., Smith, N.A., Soares da Costa, T.P., Meftahi, N., Yao, S., Harris, T.J., Tran, S.,
591 Pettikiriarachchi, A., Perugini, M.A., Keizer, D.W., Evangelista, M., Smith, B.J., Fairlie, W.D.
592 (2019) Structural insights into BCL2 pro-survival protein interactions with the key autophagy
593 regulator BECN1 following phosphorylation by STK4/MST1. Autophagy **15**, 785–795.

594 Lin, H., Chen, M., Rothe, K., Lorenzi, M.V., Woolfson, A., Jiang, X. (2014) Selective
595 JAK2/ABL dual inhibition therapy effectively eliminates TKI-insensitive CML stem/progenitor
596 cells. Oncotarget**18**, 8637–8650.

597 Liu, N., Zang, S., Liu, Y., Wang, Y., Li, W., Liu, Q., Ji, M, Ma, D., Ji, C. (2016) FZD7 regulates
598 BMSC-mediated protection of CML cells. Oncotarget **7**, 6175–6187.

599 Lowry, O.H., Rosebrough, N.J., Farr A.L., Randall R.J. (1951) Protein measurement with the
600 Folin phenol reagent. J. Biol. Chem. **193**, 265–275.

601 Mathisen, M.S., Kantarjian, H.M., Cortes, J., Jabbour, E.J. (2014) Practical issues surrounding
602 the explosion of tyrosine kinase inhibitors for the management of chronic myeloid leukemia.
603 Blood Rev. **28**, 179–187.

604 Mello, J.C., Moraes, V.W.R., Watashi, C.M., Silva, D.C.D.A., Cavalcanti, L.P., Franco,
605 M.K.K.D., Yokaichiya, F., Araujo, D., Rodrigues, T. (2016) Enhancement of chlorpromazine
606 antitumor activity by Pluronics F127/L81 nanostructured system against human multidrug
607 resistant leukemia. Pharmacol. Res. **111**, 102–112.

608 Mizushima, N., Yoshimori, T., Levine, B. (2010) Methods in mammalian autophagy research.
609 Cell **140**, 313–326.

610 Moraes, V.W., Caires, A.C., Paredes-Gamero, E.J., Rodrigues, T. (2013) Organopalladium
611 compound 7b targets mitochondrial thiols and induces caspase-dependent apoptosis in human
612 myeloid leukemia cells. Cell Death Dis, doi: 10.1038/cddis.2013.190.

613 Nourkeyhani, H., Jason, D.H.P., Scott, P., Hanekamp, D., Johnson, M., Wang, E.S. (2016)
614 Targeting autophagy as a therapeutic strategy in acute myeloid leukemia. Blood**128**, 3950.

615 Pan, X.N., Chen, J.J., Wang, L.X., Xiao, R.Z., Liu, L.L., Fang, Z.G., Liu, Q., Long, Z.J., Lin,
616 D.J. (2014) Inhibition of c-Myc overcomes cytotoxic drug resistance in acute myeloid leukemia
617 cells by promoting differentiation. PloS One. **9**, e10538.

618 Poteet, E., Choudhury, G.R., Winters, A., Li, W., Ryou, M.G., Tang, L., Ghorpade, A., Wen, Y.,
619 Yuan, F., Keir, S.T., Yan, H., Bibner, D.D., Simpkins, J.W., Yang, S.H. (2013) Reversing the
620 Warburg effect as a treatment for glioblastoma. J. Biol. Chem. **288**, 9153-9164.

621 Ravinesh, M., Swati, S., Bhartendu, S., Shubham, G., Gurpreet, K., Sweta, B., Anees, A.S., Asif,
622 H., Rajeev, K.S., Rashid, M., Kumar, D., Sati, B., Shalmati, N., Kumar, R. (2017)
623 Phenothiazines and related drugs as multi drug resistance reversal agents in cancer chemotherapy
624 mediated by P-glycoprotein. Curr. Cancer Ther. Rev.**13**, 28–42.

625 Reed, J.C. (1997) Bcl-2 family proteins: regulators of apoptosis and chemoresistance in
626 hematological malignancies. Semin. Hematol.**34**, 9–19.

627 Rieger, A.M., Nelson, K.L., Konowalchuk, J.D., Barreda, D.R. (2011) Modified annexin
628 V/propidium iodide apoptosis assay for accurate assessment of cell death. J. Vis. Exp. doi:
629 10.3791/2597.

630 Rossari, F., Minutolo, F., Orciuolo, E. (2018) Past, present, and future of Bcr-Abl inhibitors:
631 from chemical development to clinical efficacy. J. Hematol. Oncol. **11**, 84.

632 Rothfuss O., Fischer H., Hasegawa T., Maisel M., Leitner, P., Miesel, F., Sharma, M.,
633 Bornemann, A., Berg, D., Gasser, T., Patenge, N. (2009) Parkin protects mitochondrial genome
634 integrity and supports mitochondrial DNA repair. Hum. Mol. Genet. **18**, 3832-3850.

635 Slater, T.F. (1968) The inhibitory effects in vitro of phenothiazines and other drugs on lipid-
636 peroxidation systems in rat liver microsomes, and their relationship to the liver necrosis
637 produced by carbon tetrachloride. Biochem. J. **106**, 155–160.

638 Sleire, L., Førde, H.E., Netland, I.A., Leiss L., Skeie, B.S., Enger, P.Ø. (2017) Drug repurposing
639 in cancer. Pharmacol. Res. **124**, 74–91.

640 Sujobert, P., Bardet. V., Cornillet-Lefebvre P., Hayflick J.S., Prie, N., Verdier, F., Verdier, F.,
641 Vanhaesebroeck, B., Muller, O., Pesce, F., Ifrah, N., Hunault-Berger, M., Berthou, C.,
642 Villemagne, B., Jourdan, E., Audhuy, B., Solary, E., Witz, B., Harousseau, J.L., Himberlin, C.,
643 Lamy, T., Lioure, B., Cahn, J.Y., Dreyfus, F., Mayeux, P., Lacombe, C., Bouscary, D. (2005)
644 Essential role for the p110delta isoform in phosphoinositide 3-kinase activation and cell
645 proliferation in acute myeloid leukemia. Blood **106**, 1063–1066, D.

646 Tanida, I., Minematsu-Ikeguchi, N., Ueno, T., Kominami, E. (2005) Lysosomal turnover, but
647 not a cellular level, of endogenous LC3 is a marker for autophagy. Autophagy **1**, 84–91.

648 Tarkkila, P., Torn, K., Tuominen, M., Lindgren L. (1995) Premedication with promethazine and
649 transdermal scopolamine reduces the incidence of nausea and vomiting after intrathecal
650 morphine. Acta Anaesthesiol. Scand. **39**, 983–986.

651 Tolkovsky, A. (2009) Mitophagy. Biochim. Biophys. Acta **1793**, 1508–1523.

652 Tsay, M.E., Procopio, G., Anderson B.D., Klein-Schwartz W. (2015) Abuse and intentional
653 misuse of promethazine reported to US poison centers: 2002 to 2012. J. Addict Med. **9**, 233–230.

654 World Health Organization [internet].Latest global cancer data. 2018 [cited 19Jan28].

655 Wu, C.H., Bai, L.Y., Tsai, M.H., Chu, P.C., Chiu, C.F., Chen, M.Y., Chiu S.J., Chiang J., Weng,
656 J.R. (2016) Pharmacological exploitation of the phenothiazine antipsychotics to develop novel
657 antitumor agents: A drug repurposing strategy. Sci. Rep. **6**, 27540.

658 Zhang, L., Wang. Z., Khishignyam, T., Chen, T., Zhou, C., Zhang, Z., Jin, M., Wang, R., Qiu,
659 Y., Kong D. (2018) In vitro anti-leukemia activity of dual PI3K/mTOR inhibitor Voxtalisib on
660 HL60 and K562 cells, as well as their multidrug resistance counterparts HL60/ADR and
661 K562/A02 cells. Biomed. Pharmacother. **103**, 1069-1078.

662 Zhelev, Z., Ohba, H., Bakalova, R., Hadjimitova, V., Ishikawa, M., Shinohara, Y., Baba, Y.
663 (2014) Phenothiazines suppress proliferation and induce apoptosis in cultured leukemic cells
664 without any influence on the viability of normal lymphocytes. (2004) Can. Chemother.
665 Pharmacol. **53**, 267–275.

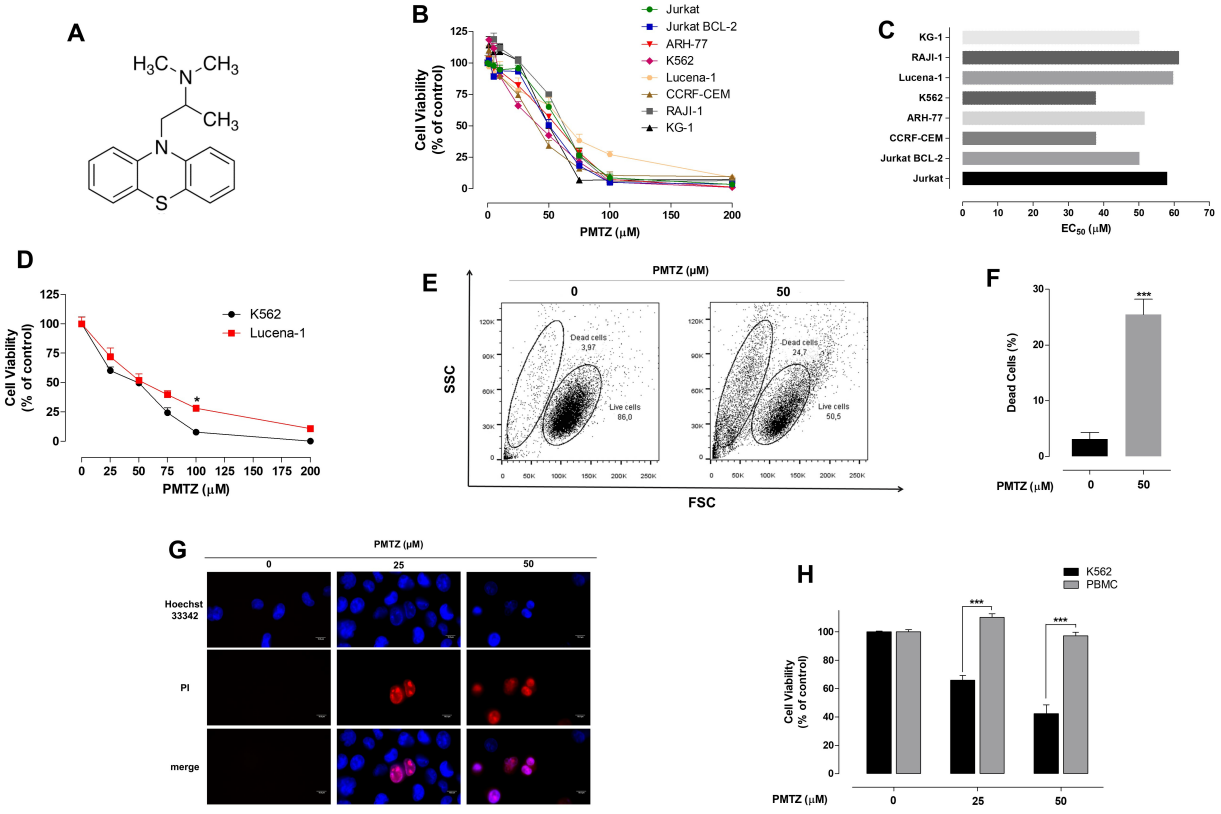

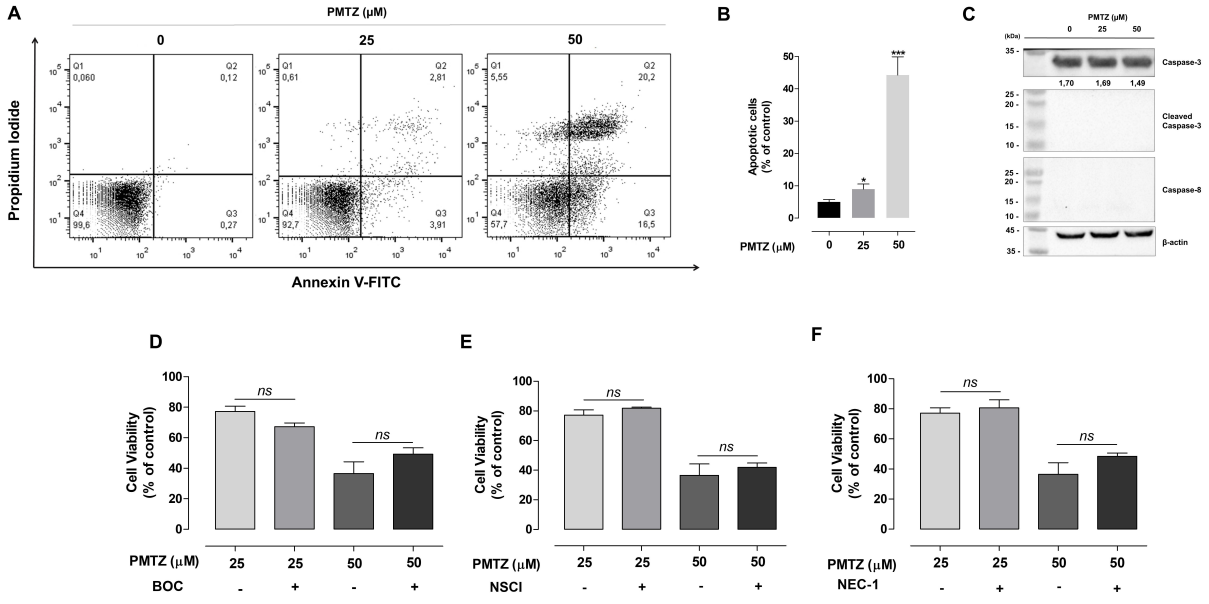

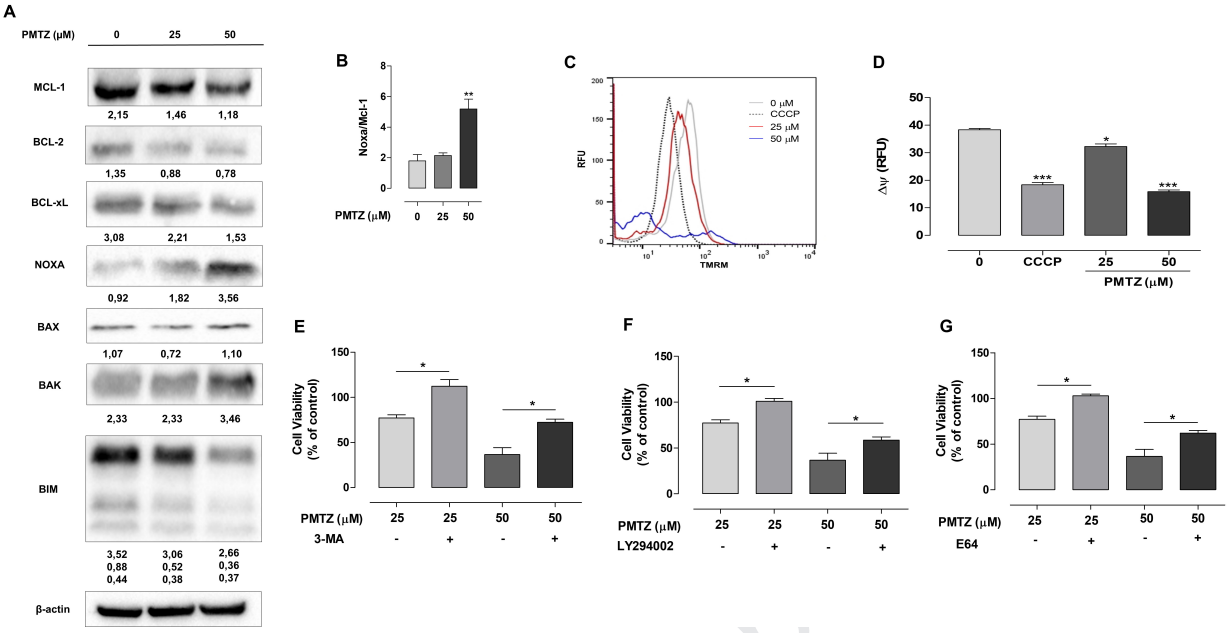

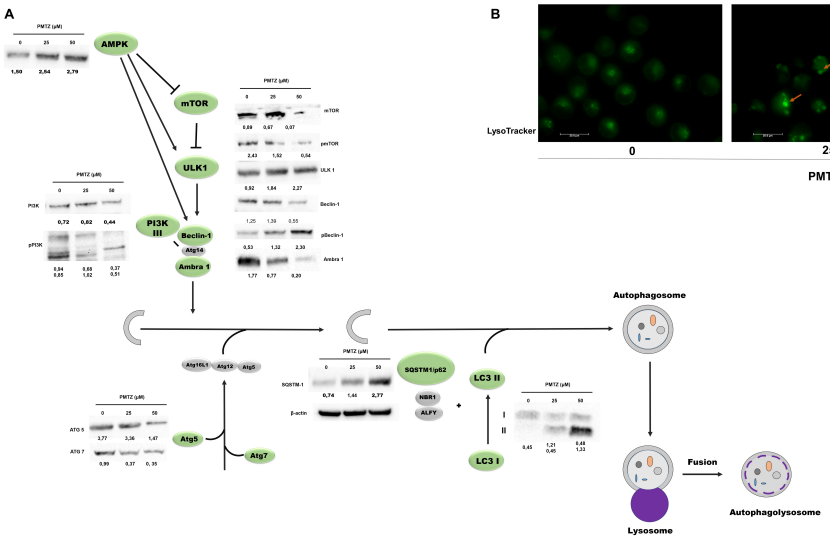

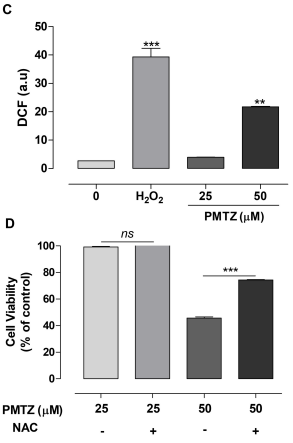

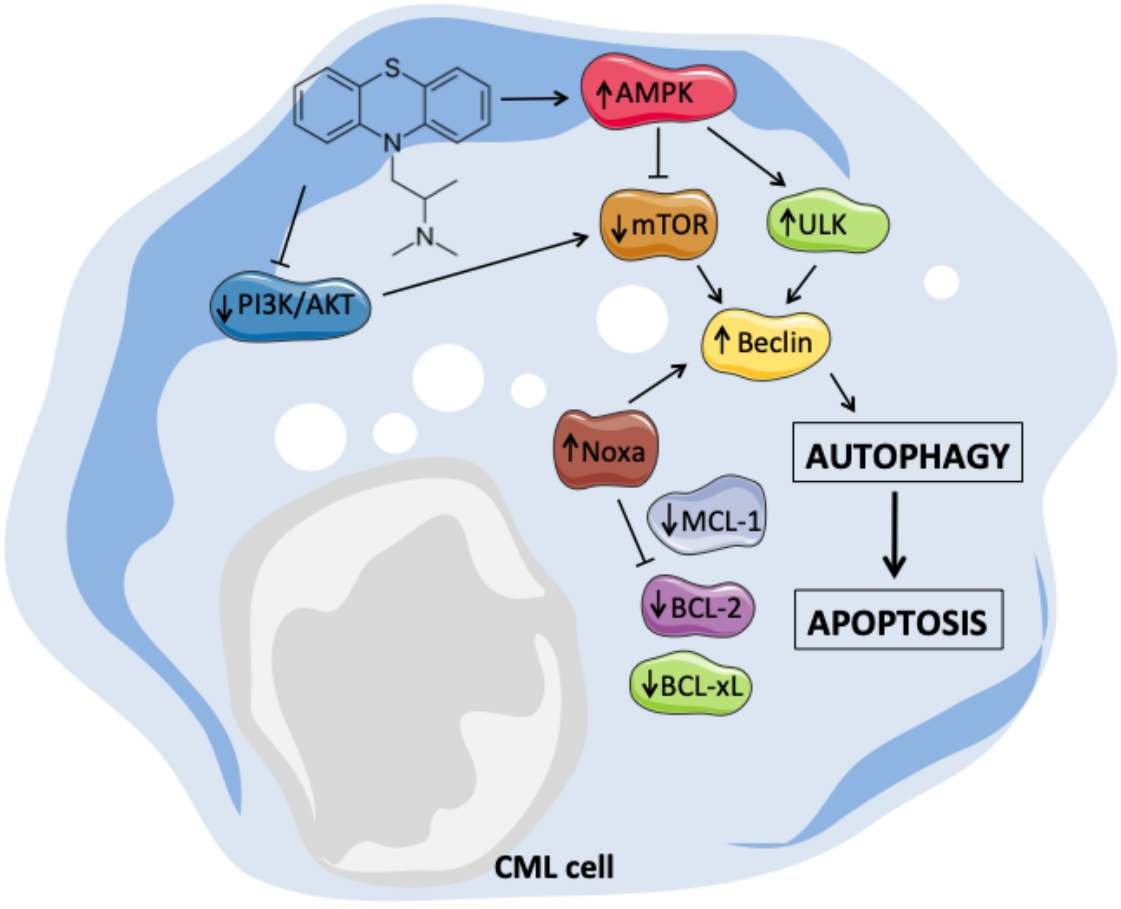
S
N
N
↑AMPK
↓mTOR
↑ULK
↓PI3K/AKT
↑Beclin
↑Noxa
AUTOPHAGY
↓MCL-1
↓BCL-2
APOPTOSIS
↓BCL-xL
CML cell

Declaration of interests

☑ The authors declare that they have no known competing financial interests or personal relationships that could have appeared to influence the work reported in this paper.